Chapter 13

Composite Structures of d-Wave and s-Wave Superconductors (d-Dot): Analysis Using Two-Component Ginzburg-Landau Equations

Masaru Kato, Takekazu Ishida, Tomio Koyama and Masahiko Machida

Additional information is available at the end of the chapter

http://dx.doi.org/10.5772/51550

1. Introduction

Superconductivity is a macroscopic quantum phenomenon [1]. Therefore it shows quite interesting properties because of its quantum nature. Such properties are described by a macroscopic complex wave function of the superconductivity. Especially, a phase of the macroscopic wave function play an important role in these properties. For example, superconducting devices, such as, superconducting charge, flux and phase qubits, superconducting single flux quantum device, and intrinsic Josephson junction Terahertz emitter of high Tc cuprate superconductors, use such quantum nature of superconductivity. They have attracted much attention recently.

In conventional superconductors, there is only single phase ϕ of the superconducting order parameter or the macroscopic wave function $\Delta = |\Delta| e^{i\phi}$. This phase causes interference effect, such as, Josephson effect, and quantization of vortices in the superconductor. But unconventional and anisotropic superconductivity have different phase that comes from internal degree of freedom of the superconducting order parameter. Because in the superconductors, electrons are paired and if their paring symmetry is an s-wave, as in the conventional superconductors, the order parameter is just a single complex number. But if the symmetry is other one such as p-wave or d-wave, then the order parameter has an internal phase [2,3]. For example, d-wave superconductors, especially $d_{x^2-y^2}$-wave superconductors have a symmetry that is shown in Fig. 1. This symmetry is internal and it appears in momentum space that means the wave function of the Cooper pair moving along the x-axis has + sign and that moving along y-axis has – sign. This is also another phase of superconducting order parameter and it affects the interference phenomena in the superconductors.

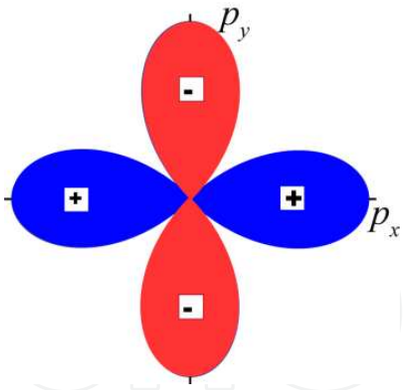

Figure 1. The symmetry of $d_{x^2-y^2}$ -wave superconductivity. The color shows the sign of wave function (order parameter) and the shape shows the amplitude of the wave function (order parameter).

The high-Tc cuprate superconductors are typical example of d-wave superconductors. Since the discovery of the high-Tc superconductors, the pairing symmetry, as well as its origin, has been controversial, but phase-sensitive experiment is crucial for determining the symmetry of the Cooper pairs. One such phase-sensitive experiment is a corner junction experiment [4,5]. In this experiment, a square-shaped high-Tc superconductor is connected with a conventional s-wave superconductor with two Josephson junctions A and B, around a corner and each junction is perpendicular to either of the x or the y axes of the high-Tc superconductor, as shown in Fig. 2.

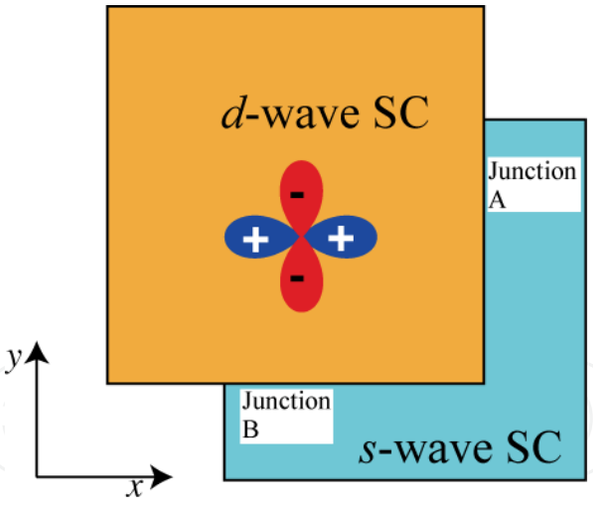

Figure 2. Configuration of corner junction between d- and s-wave superconductors. There are two junctions, A and B.

In such geometry if the Cooper pair tunnels through junction A has phase 0, then the Cooper pair tunnels through junction B has phase π. The critical current between the s- and the d-wave superconductors through these two junctions is zero under zero external magnetic field because each supercurrent cancels with each other. This is in apparent contrast with a corner junction between both s-wave superconductors for which the critical current is largest under zero external field. Therefore, from this experiment, the symmetry

of the Cooper pairs in high-Tc superconductors was determined as d-wave, especially $d_{x^2-y^2}$.

In addition, this experiment showed that the critical current become smax when the total magnetic flux through the corner junction was $\Phi_0/2$. Here, $\Phi_0 = hc/2e$ is the flux quantum. Because the phase difference π between two Josephson currents through junctions A and B, is compensated by additional phase,

$$\chi = \int_C \frac{2e}{c\hbar} A \cdot ds = \int_s \frac{2e}{c\hbar} curlA \cdot dS = 2\pi \frac{2e}{ch} \Phi = 2\pi \frac{\Phi}{\Phi_0} \quad (1)$$

where C is a contour around the corner junction and *S* is the area surrounded by the C and Φ is the total magnetic flux through the junctions. When total magnetic flux $\Phi = \Phi_0/2$, this phase becomes $\chi = \pi$. With this phase, total phase difference becomes 0 or 2π. Therefore two Josephson currents now are reinforced with each other.

This result shows, the stable superconducting state under zero external current and zero external field becomes nontrivial. For such stable state, the free energy of whole system, especially the superconducting condensation energies of both d- and s-wave superconductors should be low. Therefore the order parameter should become continuous across both of junctions. And then the phase of order parameter cannot be uniform because of the phase difference π between two junctions. This phase difference π should be compensated by changing the phase of the order parameter spatially in both s- and d-wave superconducting regions because of single valuedness of the order parameter. This spatial variation of the order parameter causes the supercurrent around the corner junction and then spontaneous magnetic flux is created at the corner without an external field. Because the associated phase change of this supercurrent is not 2π but only π, the spontaneous magnetic flux is not singly quantized magnetic flux Φ_0, but half-flux quantum magnetic flux ($\Phi_0/2$).

An experiment showing this property was done by Higenkamp et al., who made a zigzag junction between conventional s-wave superconductor Nb and high-Tc d-wave superconductor YBCO, which consists of successive corner junctions [6]. And they observed spontaneous magnetic fluxes at every corner under a zero external field, using scanning SQUID microscope. The spontaneous magnetic fluxes aligned antiferromagnetically, because of the attractive vortex-anti-vortex interaction. They also made small ring with two junctions between Nb and YBCO, which is called π-rings, and controlled the spontaneous half-quantum magnetic fluxes [7].

When spontaneous magnetic flux appears in the zero external magnetic field, this state does not have the time reversal symmetry, which the original system has. Therefore there are always two degenerate stable states. In these states, supercurrent directions are opposite and henceforth directions of spontaneous magnetic fluxes are opposite. This spontaneously appeared magnetic flux is useful and can be used as a spin or a bit by it self. Ioffe et al. [8] proposed a quantum bit using this half-quantum flux. Using the spontaneous magnetic flux

as an Ising spin system, Kirtley et al. made a frustrated triangular lattice of π-rings [7]. In their systems, the π-rings were isolated and interacted with each other purely by the electromagnetic force.

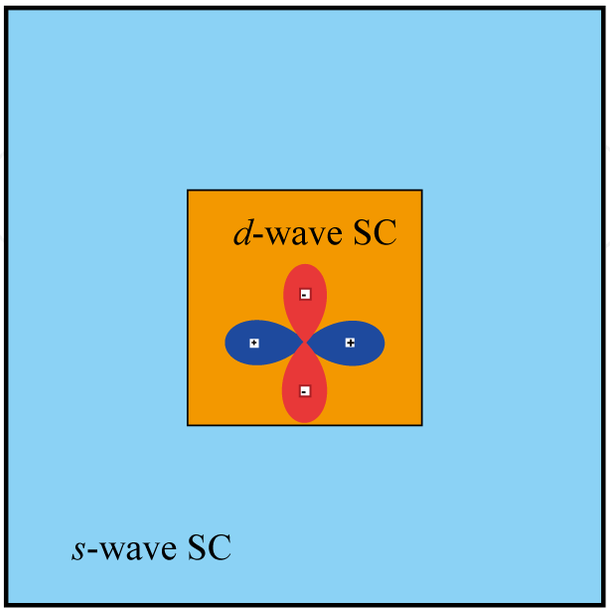

Figure 3. Schematic diagram of a d-dot.

In contrast to the previous approach for using the spontaneous half-flux quantum, we considered nano-sized d-wave superconductor embedded in an s-wave matrix, as shown in Fig. 3 [9-11]. We want to consider the whole d-dot system as a single element, not the individual half-quantum fluxes. As in the single half-quantum system, our d-dot has two degenerate states if the spontaneous magnetic fluxes appear, because the state with spontaneous magnetic fluxes under zero external field also breaks time-reversal symmetry. This property is independent from the shape, and the d-dot in any shape always has two degenerate stable states. Therefore, the d-dot as a whole can be considered as a single element with two level states and it might be used as a spin or a bit also as a qubit. It has better properties than those of single flux quantum element, which will be shown in following sections.

In the following, we first show a phenomenological superconducting theory, which describes the spontaneous magnetic fluxes in these composite structures, especially in d-dot systems and then we discuss the basic properties of this d-dot, based on this phenomenological theory. Also, we discuss the difference between a single half-quantum flux system and our d-dot system.

2. Model: two components Ginzburg-Landau free energy

In order to discuss the basic properties of the d-dot, especially to describe the appearance of spontaneous magnetic fluxes, we use the phenomenological Ginzburg-Landau (GL) theory. However, for anisotropic superconductors, such as the $d_{x^2-y^2}$-wave high-Tc cuprate

superconductors, their anisotropy cannot be treated by the simple GL theory. This is because using only up to quartic term and quadratic term of gradients of the single order parameters in free energy, there are no anisotropic terms. Anisotropy of the vortices in d-wave superconductors within the phenomenological theory was treated by Ren et al., who used a two-component GL theory [12-15]. Here, two components mean the two components of the order parameter of with s and d symmetries. They derived the two-component GL free energy from the Gor'kov equations.

Multi-components GL equations were used for exotic superconductors, e.g. heavy fermion superconductors[16-18] and Sr_2RuO_4[19,20]. Also, recently, two components GL equations are studied for two-band or two-gap superconductors, such as MgB_2 [21,22].

The model by Ren.et al. especially emphasize the anisotropy of d-wave superconductivity. Therefore, we use the following two-component Ginzburg-Landau (GL) free energy for d-wave superconductors;

$$\begin{aligned} \mathsf{F}_d(\Delta_s,\Delta_d,\mathbf{A}) = \int_\Omega \Bigg(& \frac{3\alpha}{8}\lambda_d\left[|\Delta_d|^2 - \frac{4\ln(T_{cd}/T)}{3\alpha}\right]^2 + \alpha\lambda_d\left[|\Delta_s|^4 + 2\frac{\alpha_s}{\alpha}|\Delta_s|^2\right] \\ & + \frac{1}{4}\alpha\lambda_d v_F^2\left[\left|\boldsymbol{\Pi}\Delta_d^*\right|^2 + 2\left|\boldsymbol{\Pi}\Delta_s\right|^2 + \left(\Pi_x^*\Delta_s\Pi_x\Delta_d^* - \Pi_y^*\Delta_s\Pi_y\Delta_d^* + \text{H.c.}\right)\right] \\ & + \alpha\lambda_d\left[2|\Delta_s|^2|\Delta_d|^2 + \frac{1}{2}\left(\Delta_s^{*2}\Delta_d^2 + \Delta_s^2\Delta_d^{*2}\right)\right] + \frac{1}{8\pi}\left[|\mathbf{h}-\mathbf{H}|^2 + (\operatorname{div}\mathbf{A})^2\right]\Bigg) d\Omega \end{aligned} \tag{2}$$

where $\Pi = \frac{\hbar}{i}\nabla - \frac{2e}{c}\mathbf{A}$ is a generalized momentum operator that is gauge invariant and $\alpha = \frac{7\zeta(3)}{8(\pi T)^2}$. Δ_d and Δ_s are the d-wave and the s-wave components of the order parameter, respectively. $\lambda_d = V_d N(0)$ is the strengths of the coupling constants for the d-wave interaction channel and $\alpha_s = \frac{1+\frac{V_s}{V_d}}{\lambda_d}$. Here, $N(0)$ is the density of states of electrons at the Fermi energy and V_d and V_s are interaction constants between electrons for d- and s-wave channels, respectively. We assume attractive and repulsive interactions for the d- and the s-wave channels, respectively. T_{cd} is the transition temperature of the d-wave superconductivity under zero-external field. $\mathbf{H}$ is an external field and $\mathbf{h} = \operatorname{curl}\mathbf{A}$. We take the London gauge i.e. $\nabla\cdot\mathbf{A} = 0$ and $\mathbf{A}\cdot\mathbf{n} = 0$ at the surface of superconductor. The term $(\nabla\cdot\mathbf{A})^2$ in the integrand of Eq. 2 is added for fixing the gauge.

Also, for s-wave superconductors, we use the following two-component GL equation with attractive and repulsive interactions for the s-wave and the d-wave channels, respectively:

$$\begin{aligned} \mathsf{F}_s\left(\Delta_s,\Delta_d,\mathbf{A}\right) &= \int_\Omega\left(\frac{\alpha}{2}\lambda_s\left[\left|\Delta_s\right|^2-\frac{\ln\left(T_{cs}/T\right)}{\alpha}\right]^2+\frac{\alpha\lambda_s}{2}\left[\frac{3}{8}\left|\Delta_d\right|^4+\frac{\alpha_d}{\alpha}\left|\Delta_d\right|^2\right]\right. \\ &+\frac{1}{8}\alpha\lambda_s v_F^2\left[\left|\mathbf{\Pi}\Delta_d^*\right|^2+2\left|\mathbf{\Pi}\Delta_s\right|^2+\left(\Pi_x^*\Delta_s\Pi_x\Delta_d^*-\Pi_y^*\Delta_s\Pi_y\Delta_d^*+\text{H.c.}\right)\right] \\ &\left.+\frac{\alpha\lambda_s}{2}\left[2\left|\Delta_s\right|^2\left|\Delta_d\right|^2+\frac{1}{2}\left(\Delta_s^{*2}\Delta_d^2+\Delta_s^2\Delta_d^{*2}\right)\right]+\frac{1}{8\pi}\left[\left|\mathbf{h}-\mathbf{H}\right|^2+\left(\nabla\cdot\mathbf{A}\right)^2\right]\right)d\Omega \end{aligned} \tag{3}$$

Here $\lambda_s = V_s N(0)$ is the strengths of the coupling constants for the s-wave interaction channeland $\alpha_d = \dfrac{2\frac{V_s}{V_d}-1}{\lambda_s}$.

In these free energies, the anisotropy of the d-wave superconductivity appears in the coupling terms of the gradient of both components of order parameters, $\left(\Pi_x^*\Delta_s\Pi_x\Delta_d^*-\Pi_y^*\Delta_s\Pi_y\Delta_d^*+\text{H.c.}\right)$, where the two terms that contain the gradients along the x and the y directions have different signs.

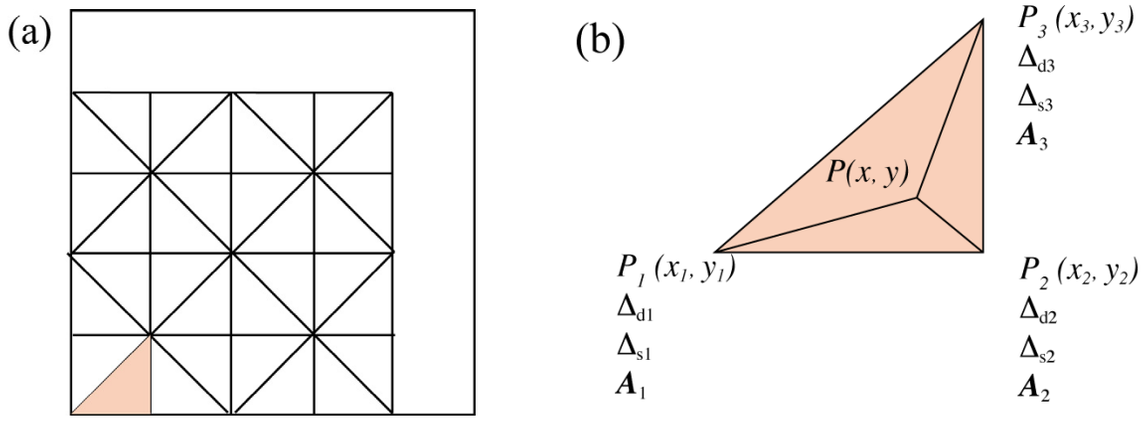

Figure 4. (a) Triangle elements of superconductors. (b) Nodes of a triangle element and the value of physical quantities at the nodes.

By minimizingthe sum of these free energies, we obtain the Ginzburg-Landau (GL) equations. For this purpose, we use the finite-element method [23-25], because we want to investigate variously shaped d-dots. Hereafter we consider two-dimensional system and ignore the variation of physical quantities along the direction perpendicular to the two dimensional system. In the finite-element method for two-dimensional system, we divide the superconductor region into small triangular elements (see Fig. 4 (a)) and then expand the order parameters and the vector potential in each element by using the area coordinate, which is defined as,

$$N_i^e\left(x,y\right)=\begin{cases}\dfrac{1}{2S_e}\left(a_i+b_i x+c_i y\right) & \text{inside of element}\\ 0 & \text{outside of element}\end{cases}\qquad \left(\text{i}=1,2,3\right) \tag{4}$$

S_e is an area of e-th element and the coefficients are defined as,

$$a_i = x_j^e y_k^e - x_k^e y_j^e \tag{5}$$

$$b_i = y_j^e - y_k^e \tag{6}$$

$$c_i = x_k^e - x_j^e \tag{7}$$

where (i, j, k) is a cyclic permutation of $(1,2,3)$ and (x_i^e, y_i^e) is the coordinate of the i-th nodes of the e-th element (see Fig. 4(b)).These area coordinates are localized functions as shown in Fig. 5.Also the area coordinate $N_i^e(x, y)$ represents normalized area of a triangular of which nodes are P, P_j and P_k in Fig. 5 (b), where (i, j, k) is a cyclic permutation of $(1,2,3)$. And then they have following properties;

$$\sum_{i=1}^{3} N_i^e(x, y) = 1 \tag{8}$$

$$N_i^e(x_j^e, y_j^e) = \delta_{ij} \tag{9}$$

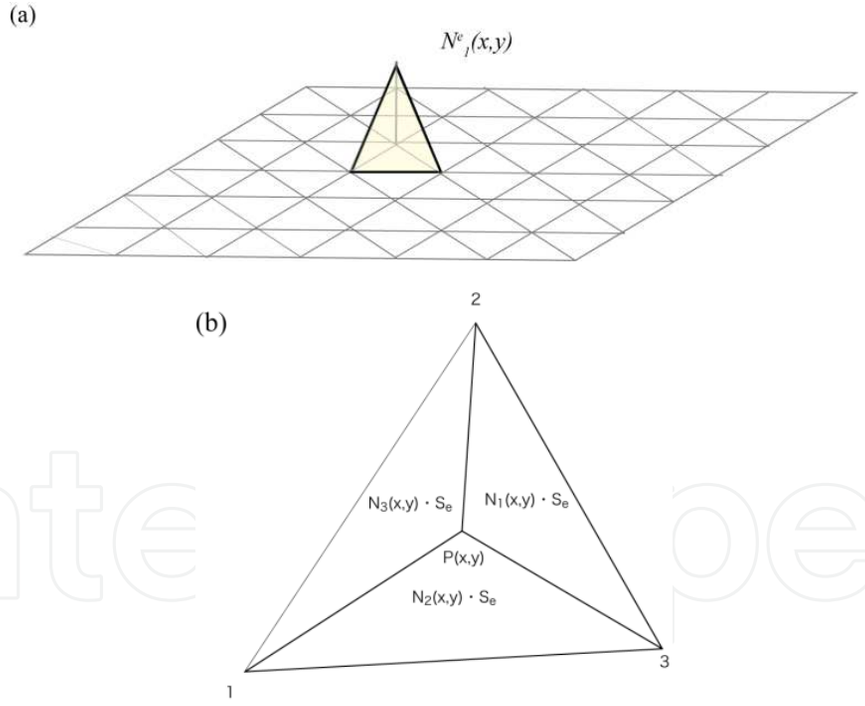

Figure 5. (a) A bird's-eye view of an area coordinate $N_i^e(x, y)$. (b) Area coordinates represent normalized area of triangular elements.

Using these properties, the order parameters are expanded as

$$\Delta_d(x, y) = \sum_e \sum_{i=1}^{3} \Delta_{di}^e N_i^e(x, y) \tag{10}$$

$$\Delta_s(x,y)=\sum_e\sum_{i=1}^{3}\Delta_{si}^e N_i^e(x,y) \tag{11}$$

and also the magnetic vector potential is expanded as,

$$\mathbf{A}(x,y)=\sum_e\sum_{i=1}^{3}\mathbf{A}_i^e N_i^e(x,y) \tag{12}$$

where Δ_{di}^e and Δ_{si}^e are the value of the d-wave and the s-wave order parameters at the i-th vertex of e-th element, respectively (see Fig. 4 (b)). Also, $\mathbf{A}_i^e$ is the value of the vector potential at the i-th vertex of the e-th element (see Fig. 4 (b)). Inserting these expansions into the free energies Eqs. 2 and 3, the free energies are expressed by those values, Δ_{di}^e, Δ_{si}^e and $\mathbf{A}_i^e$. Then, minimizing the free energies, we get following GL equations. For the d-wave superconducting order parameter,

$$\begin{aligned}&\sum_j\left[P_{ij}^{dd}(\{A\})+P_{ij}^{dd2R}(\{\Delta\})\right]\mathrm{Re}\,\Delta_{dj}+\sum_j\left[Q_{ij}^{dd}(\{A\})+Q_{ij}^{dd2}(\{\Delta\})\right]\mathrm{Im}\,\Delta_{dj}\\&+\sum_j P_{ij}^{ds}(\{A\})\,\mathrm{Re}\,\Delta_{sj}+\sum_j Q_{ij}^{ds}(\{A\})\,\mathrm{Im}\,\Delta_{sj}=V_i^{dR}(\{\Delta\})\end{aligned} \tag{13}$$

$$\begin{aligned}&\sum_j\left[-Q_{ij}^{dd}(\{A\})+Q_{ij}^{dd2}(\{\Delta\})\right]\mathrm{Re}\,\Delta_{dj}+\sum_j\left[P_{ij}^{dd}(\{A\})+P_{ij}^{dd2I}(\{\Delta\})\right]\mathrm{Im}\,\Delta_{dj}\\&+\sum_j P_{ij}^{ds}(\{A\})\,\mathrm{Im}\,\Delta_{sj}-\sum_j Q_{ij}^{ds}(\{A\})\,\mathrm{Re}\,\Delta_{sj}=V_i^{dI}\end{aligned} \tag{14}$$

And for the s-wave superconducting order parameter,

$$\begin{aligned}&\sum_j\left[P_{ij}^{ss}(\{A\})+P_{ij}^{ss2R}(\{\Delta\})\right]\mathrm{Re}\,\Delta_{sj}+\sum_j\left[Q_{ij}^{ss}(\{A\})+Q_{ij}^{ss2}(\{\Delta\})\right]\mathrm{Im}\,\Delta_{sj}\\&+\sum_j P_{ij}^{ds}(\{A\})\,\mathrm{Re}\,\Delta_{dj}+\sum_j Q_{ij}^{ds}(\{A\})\,\mathrm{Im}\,\Delta_{dj}=V_i^{sR}(\{\Delta\})\end{aligned} \tag{15}$$

$$\begin{aligned}&\sum_j\left[-Q_{ij}^{ss}(\{A\})+Q_{ij}^{ss2}(\{\Delta\})\right]\mathrm{Re}\,\Delta_{sj}+\sum_j\left[P_{ij}^{ss}(\{A\})+P_{ij}^{ss2I}(\{\Delta\})\right]\mathrm{Im}\,\Delta_{sj}\\&+\sum_j P_{ij}^{ds}(\{A\})\,\mathrm{Im}\,\Delta_{dj}-\sum_j Q_{ij}^{ds}(\{A\})\,\mathrm{Re}\,\Delta_{dj}=V_i^{sI}(\{\Delta\})\end{aligned} \tag{16}$$

Coefficients for d-wave region and s-wave region are different and are given in Appendix.

Also for the vector potential following equations are obtained as follows,

$$\sum_j\left[R_{ij}^e(\{\Delta_d,\Delta_s\})+R_{ij}^{2e}(\{\Delta_d,\Delta_s\})\right]A_{jx}+\sum_j S_{ij}^e A_{jy}=T_i^{ex}-T_i^{2ex}-U_i^{ey} \tag{17}$$

$$\sum_j\left[R_{ij}^e(\{\Delta_d,\Delta_s\})-R_{ij}^{2e}(\{\Delta_d,\Delta_s\})\right]A_{jy}-\sum_j S_{ij}^e A_{jx}=T_i^{ey}+T_i^{2ey}-U_i^{ex} \tag{18}$$

Here coefficients are also given in Appendix. At the boundary of d- and s-wave superconductors, because the wave function is continuous, following boundary conditions are applied:

$$\frac{\Delta_{1s}}{V_{1s}} = \frac{\Delta_{2s}}{V_{2s}} \tag{19}$$

$$\frac{\Delta_{1d}}{V_{1d}} = \frac{\Delta_{2d}}{V_{2d}} \tag{20}$$

In this model, d- and s-wave components of the order parameter interfere anisotropically with each other in the both of d-wave and s-wave superconductors. And the boundaries between both superconductors are assumed clean. But we cannot take into account the roughness of the boundary.

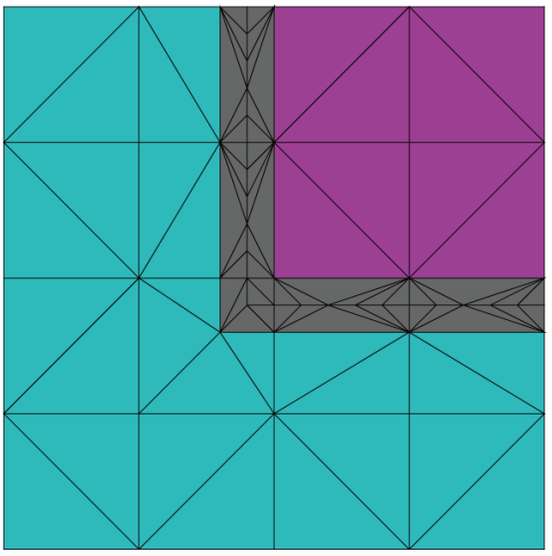

Figure 6. Mesh partition used in the finite element method. Red, blue and grey regions are d-wave and s-wave superconducting and junction regions, respectively.

For treating roughness of the junctions, we consider second model. In contrast to the first model, in the second model, the s-wave superconductor is connected to the d-wave superconductor through a thin metal or an insulator layers. In the second model, we consider only the d-wave (s-wave) component of the order parameter in the d-wave (s-wave) superconducting region, but in the thin metal layer, we take both components. So, free energies are given as,

$$\mathsf{F}_d(\Delta_d, \mathbf{A}) = \int_\Omega \left(\frac{3\alpha}{8}\lambda_d \left[|\Delta_d|^2 - \frac{4\ln T_{cd}/T}{3\alpha} \right]^2 + \frac{1}{4}\alpha\lambda_d v_F^2 \left| \mathbf{\Pi}\Delta_d^* \right|^2 + \frac{1}{8\pi}|\mathbf{h}-\mathbf{H}|^2 + \frac{1}{8\pi}(\operatorname{div}\mathbf{A})^2 \right) d\Omega \tag{21}$$

$$\mathsf{F}_s(\Delta_s, \mathbf{A}) = \int_\Omega \left(\frac{\alpha}{2}\lambda_s \left[|\Delta_s| - \frac{\ln T_{cs}/T}{\alpha} \right]^2 + \frac{1}{4}\alpha\lambda_s v_F^2 \left| \mathbf{\Pi}\Delta_s^* \right|^2 + \frac{1}{8\pi}|\mathbf{h}-\mathbf{H}|^2 + \frac{1}{8\pi}(\operatorname{div}\mathbf{A})^2 \right) d\Omega \tag{22}$$

$$\mathsf{F}_M(\Delta_s,\Delta_d,\mathbf{A})=\int_\Omega\Bigg(|\lambda_d|\frac{3b}{2}\left[|\Delta_d|^2+\frac{a_d}{3b}\right]^2+b\left[|\Delta_s|^2+\frac{a_s}{2b}\right]^2|\lambda_d|+b|\lambda_d|\Big[2|\Delta_s|^2|\Delta_d|^2+\frac{1}{2}\left(\Delta_s^{*2}\Delta_d^2+\Delta_s^2\Delta_d^{*2}\right)$$
$$+\frac{1}{4}v_F^2\left\{\left|\boldsymbol{\Pi}\Delta_d^*\right|^2+2\left|\boldsymbol{\Pi}\Delta_s^*\right|^2+\left(\Pi_x^*\Delta_s\Pi_x\Delta_d^*-\Pi_y^*\Delta_s\Pi_y\Delta_d^*+\text{H.c.}\right)\right\}\Big]+\frac{1}{8\pi}|\mathbf{h}-\mathbf{H}|^2+\frac{1}{8\pi}(\text{div}\,\mathbf{A})^2\Bigg)d\Omega \tag{23}$$

Here $\mathsf{F}_d(\Delta_d,\mathbf{A})$, $\mathsf{F}_s(\Delta_s,\mathbf{A})$ and $\mathsf{F}_M(\Delta_s,\Delta_d,\mathbf{A})$ are the free energies for d-wave, s-wave superconducting and junction regions respectively. A typical division of superconducting region to d- and s-wave superconducting and junction regions is given in Fig. 6. In the junction region, order parameters and the vector potential vary rapidly and therefore smaller mesh sizes are taken. At the boundary, we assume that each component of the order parameter is continuous.

3. Appearance of the half-quantum magnetic flux in d-dot

Using the two models in Section 2, the spontaneous magnetic flux can be described. In Fig.7, the s-wave and d-wave order parameters and magnetic field distribution are shown for a corner junction between s-wave and d-wave superconductors under zero external magnetic field.

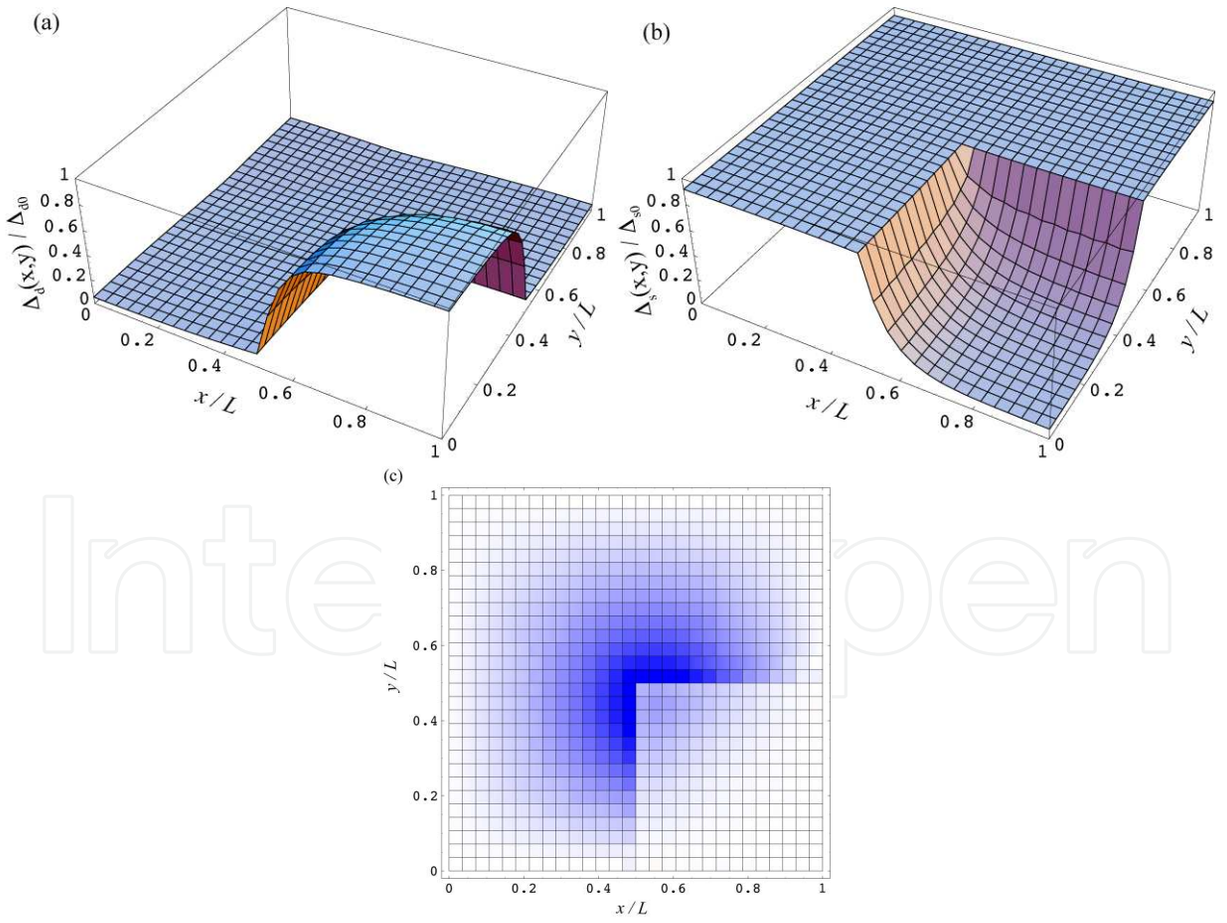

Figure 7. Appearance of spontaneous half-quantum magnetic flux at a corner junction. (a) Amplitude of s-wave component of order parameter. (b) Amplitude of s-wave component of order parameter. (c) Magnetic field distribution at zero external field.

In this calculation, the physical parameters, such as the GL parameters and the transition temperatures, for Nb and YBCO in the s- and the d-wave superconducting regions are used, and system size is set as $L = 25\xi_{d0}$. Here, ξ_{d0} is the coherence length of the d-wave superconductors at zero temperature. In Fig.7 (c), right-lower part is the d-wave superconductor and other part is s-wave superconductor. Both components of the order parameter exist in both of s- and d-wave superconductors. Especially, s-wave component penetrates into the d-wave superconducting region and interferes with d-wave component. Such interference causes the spontaneous magnetic field, which is perpendicular to the plane. In Fig. 7 (c), blue color means magnetic field H_z is positive. Total magnetic flux around the corner is approximately $\Phi_0/2$. So a half-quantum magnetic flux appears spontaneously. In this figure, the size of d-wave superconductor is $10\xi_{d0} \times 10\xi_{d0}$. The coherence length of high-Tc superconductors is rather small ($\xi_{d0} = 2 \sim 4$ nm for YBCO) and the size of d-wave region is 40 nm, which is rather small compare to the experiments by Hilgencamp et al. [6]. But for such nano-sized d-wave superconductors, half-quantum magnetic fluxes appear, as this result shows. For larger d-wave region, the spontaneous magnetic flux is expected to appear easily.

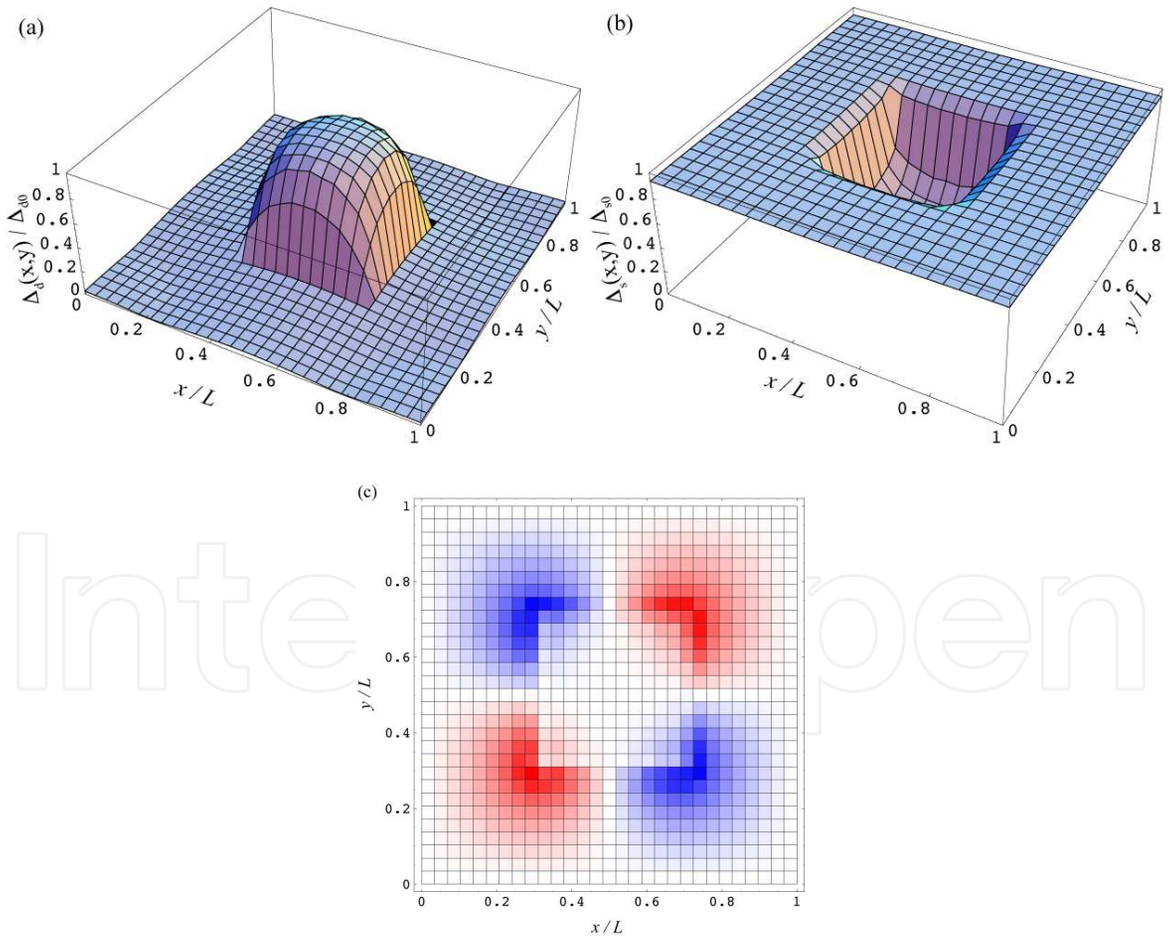

Figure 8. Superconducting order parameter and magnetic field structures for a square d-wave superconductor in an s-wave superconductor. (a) Amplitude of d-wave component of the order parameter. (b) Amplitude of s-wave component of the order parameter. (c) Magnetic field distribution. Blue means $H_z < 0$.

How such spontaneous magnetic flux appears, when a square d-wave superconductor is embedded in an s-wave superconductor? In Fig.8, the typical magnetic flux structure of such square d-dot in which edge of square is parallel to the x- or y-directions, under zero magnetic field is shown. In this figure, red color means $H_z < 0$. Magnetic fluxes appear at four corners of the square d-dot, and they order antiferromagnetically. Such antiferromagnetic order is already obtained by the experiment for zigzag junctions by Hilgencamp et al. [6]. The reason of this antiferromagnetic order can be understood by considering the interaction between vortices. Usual theory of vortex interaction tells us that parallel vortices repel each other and antiparallel vortices attract each other because of the current around the vortices and Lorentz force by this current. For the d-dot in Fig.8, the spontaneous current flows form top-center of the d-wave superconductors, turns right and left and flows into left and right sides of d-wave superconductor. So this current naturally creates upward flux at the left-top corner and downward flux at the right-top corner. Fluxes at the lower two corners can be explained similarly.

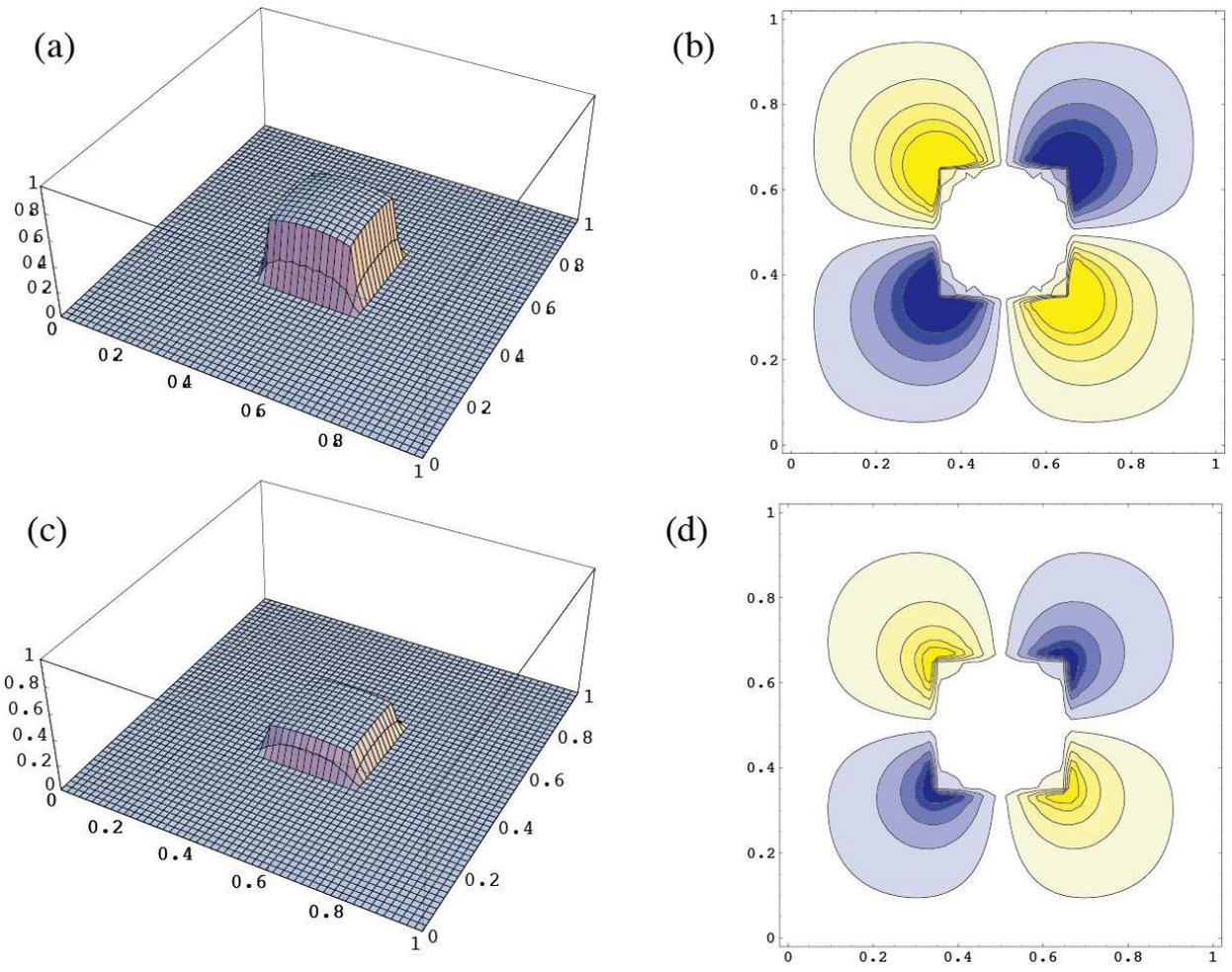

Figure 9. The d-wave superconducting order parameter amplitudes ((a) and (c)) and magnetic field distribution ((b) and (c)) for smaller d-dot with d=1.7 ξ . ((a) and (b)) with d=1.3 ξ . ((c) and (d)).

The second model of d-dots (Eqs.21-23) also describes these spontaneous half-quantum magnetic fluxes. Using this model, we argue the size-dependence of these magnetic fluxes. Question is: The d-dot in Fig.8 have four half-quantum magnetic fluxes, but if the size of d-dot becomes small, then what happens? In Fig.9, the typical size dependences of the order parameter structure and the magnetic fluxes are shown. In these figures, for smaller d-dots the amplitudes of d-wave order parameter and magnetic field distributions are shown. When the size of the d-dot becomes small, then the amplitude of d-wave component of the order parameter becomes small, and the spontaneous magnetic field becomes small. This is because the spontaneous current, which flows around each corner, does not decrease much at the center of the edge of the square when the size of the d-dot is comparable to the coherence length. Then, the total magnetic flux becomes less than the half-flux quantum, although the fluxoid is still a half-flux quantum.

The temperature dependences of amplitude of order parameters and the spontaneous magnetic fluxes also show similar tendency, because in this case, the coherence length increases with increasing temperature.

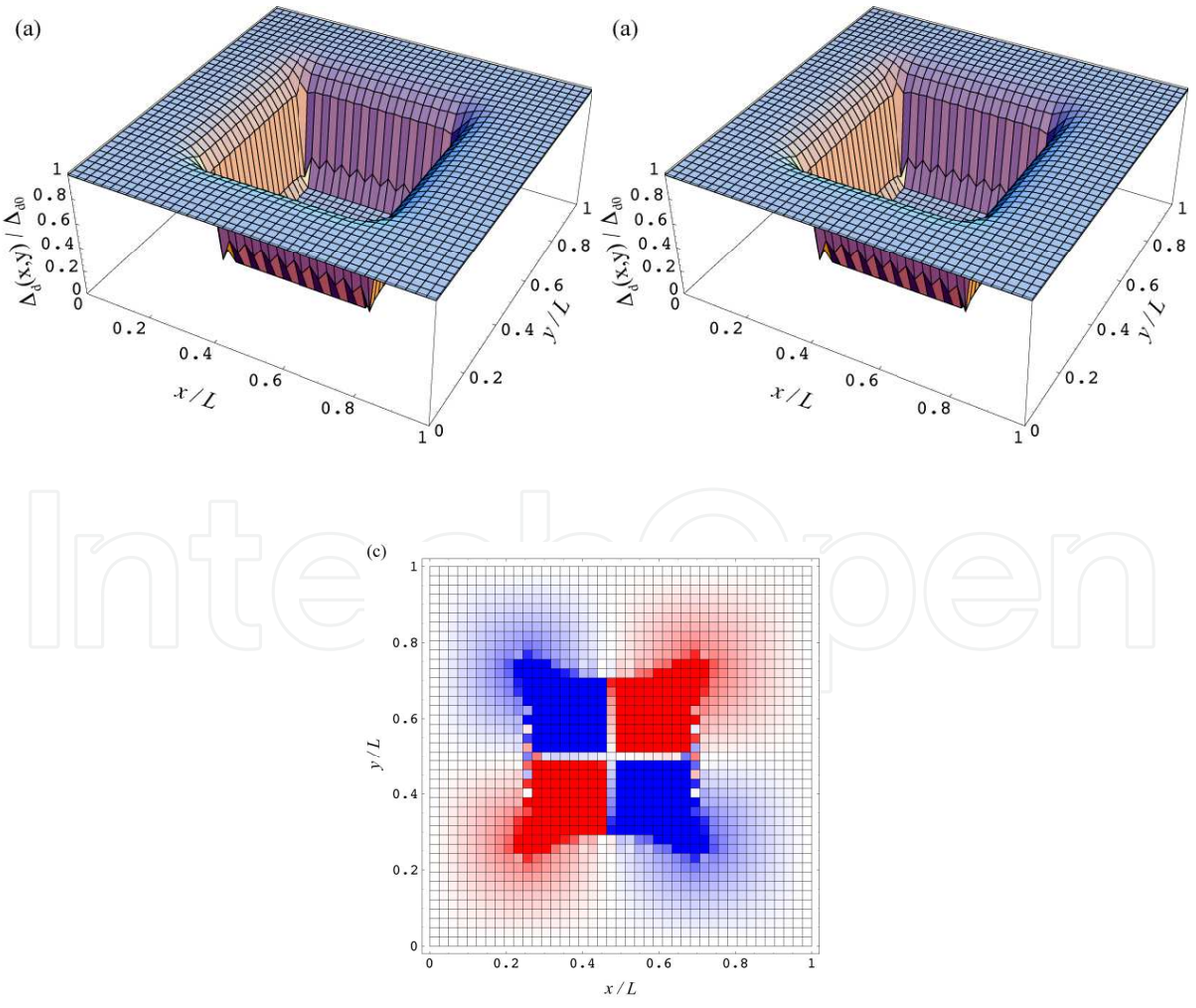

Figure 10. Order parameter ((a) d-wave and (b) s-wave) and magnetic field (c) distribution for an s-dot.

These spontaneous magnetic fluxes do not appears for the geometry for a square d-wave superconductor embedded in an s-wave superconducting matrix, but they appear for a square s-wave superconductor embedded in d-wave superconducting matrix and various shaped d-wave superconductors embedded in the s-wave superconducting matrix. The s-wave superconducting dot case is called "s-dot". For an s-dot, order parameter structures and field distribution are shown in Fig. 10. There appear spontaneous magnetic fluxes around the corners antiferromagnetically. These magnetic fluxes also are explained similarly by the phase anisotropy of d-wave superconductivity. But the distribution of magnetic field is opposite to the d-dot case, where magnetic field appears mainly outside of inner superconducting region, but in this case, magnetic field appears mainly inside of inner superconducting region. The s-dot is also useful but in the following we focus on the d-dot case, which is more easily fabricated, we think.

Next we discuss the shape dependence of the d-dot. Even if the shape of the d-wave superconducting region is different from the square that is parallel to the crystal axis or x- and y-axis, the spontaneous magnetic field is also expected. In Fig. 11, distributions of the order parameters and magnetic field for an equilateral triangle plate are shown. For this case the spontaneous magnetic fluxes appear along the upper edges connected to the top corner. The spontaneous current flows the top corner and return to the intermediate points of upper edges. Also spontaneous magnetic fluxes appear around the lower corners. These spontaneous magnetic field along the edge also appear for rotated or diagonal squares, as shown in Fig. 12. In these figures, the spontaneous currents across the junction mainly flow along x- or y- directions. And direction of junction between d- and s-wave superconductors is important for the appearance of magnetic flux.

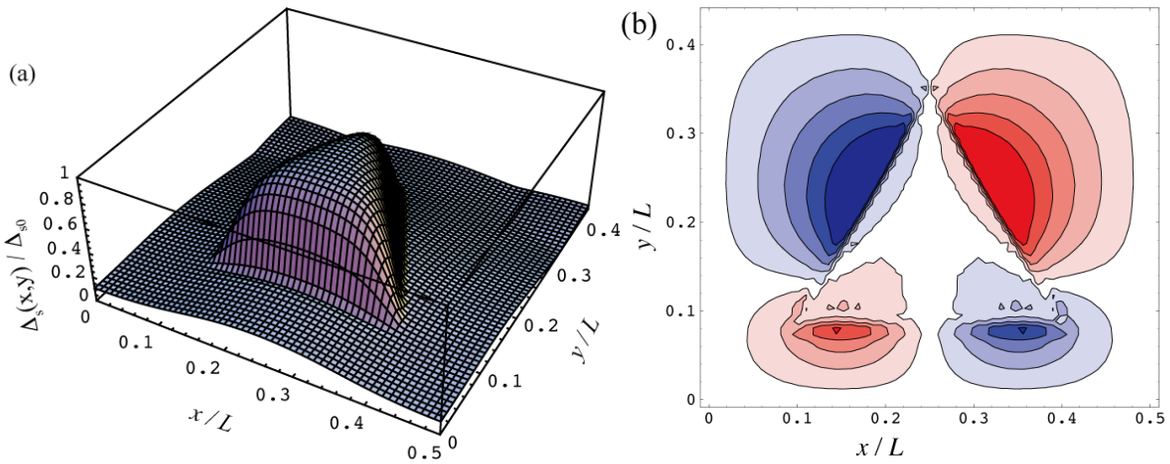

Figure 11. Spatial distribution of d-wave component of the order parameter (a) and magnetic field for a triangular d-dot.

Also we note that not only square d-dots that is parallel to the x- and y-axis but also arbitrary shaped d-dots that show spontaneous magnetic field, such as in Figs. 11 and 12, have doubly degenerate stable states. And the shape of d-dot controls 15 the magnetic field distribution.

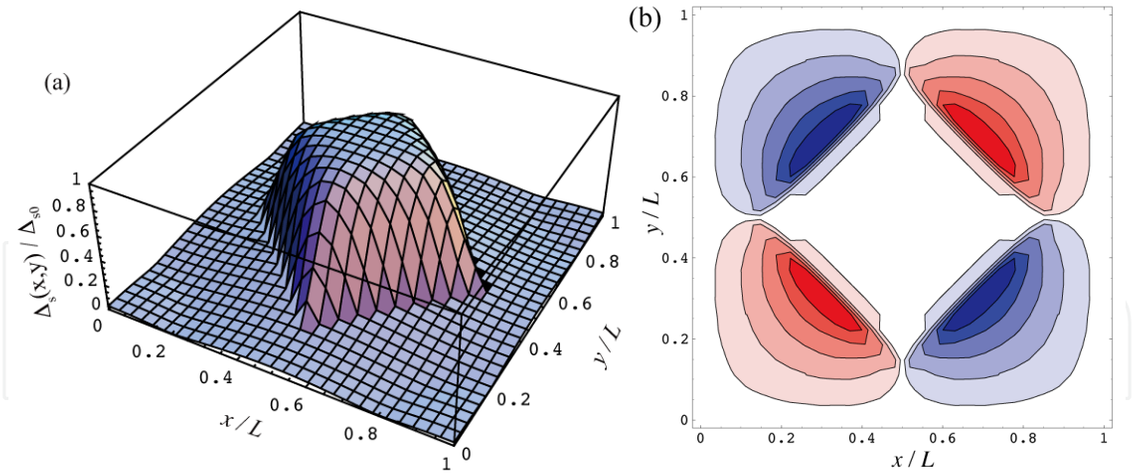

Figure 12. Spatial distribution of d-wave component of the order parameter (a) and magnetic field for a rotated square d-dot.

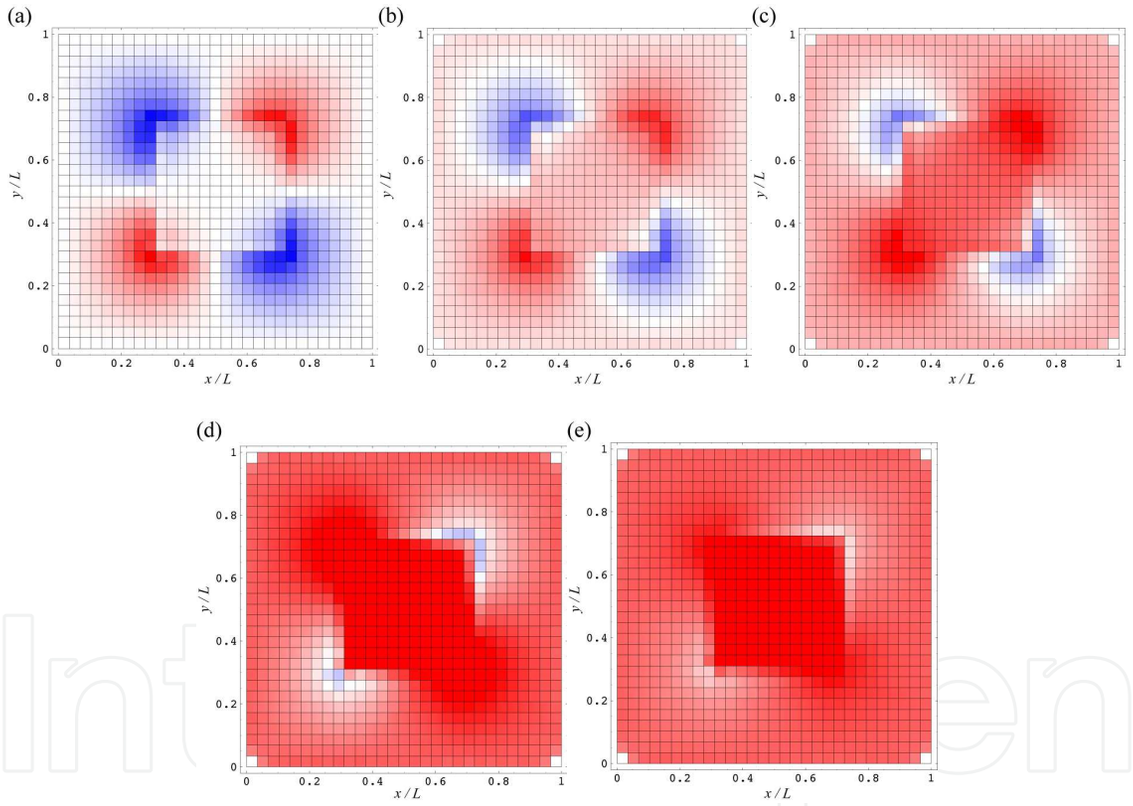

Figure 13. Spatial distribution of magnetic field for a square d-dot. (a) $H = 0$, (b) $H = 0.02\Phi_0/2\pi L^2$, (c) $H = 0.05\Phi_0/2\pi L^2$, (d) $H = 0.1\Phi_0/2\pi L^2$, and (e) $H = 0.2\Phi_0/2\pi L^2$.

These doubly degenerate states have good properties for applications. First they remain under weak external magnetic field. In Fig. 13, external field dependence of spontaneous magnetic field distributions for a square d-dot is shown. The spontaneous magnetic flux parallel (anti-parallel) to the external field becomes large (small), respectively. Although the degeneracy from broken time reversal symmetry is lifted under the external magnetic field,

the state with π/2 rotated magnetic field distributions are equally stable. These doubly degenerate states come from the broken four-fold symmetry of the square shape. This property depends on the shape of d-dots. For asymmetric shaped d-dots, one of the doubly degenerate states becomes more stable than another state. This means that we can control these degenerate states using the magnetic field for asymmetric d-dots.

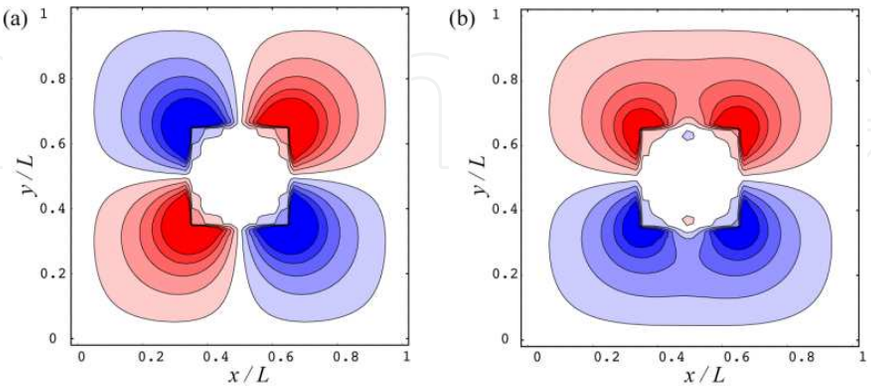

Figure 14. Magnetic field distributions of (a) the most stable state (udud) and (b) an excited state (udud).

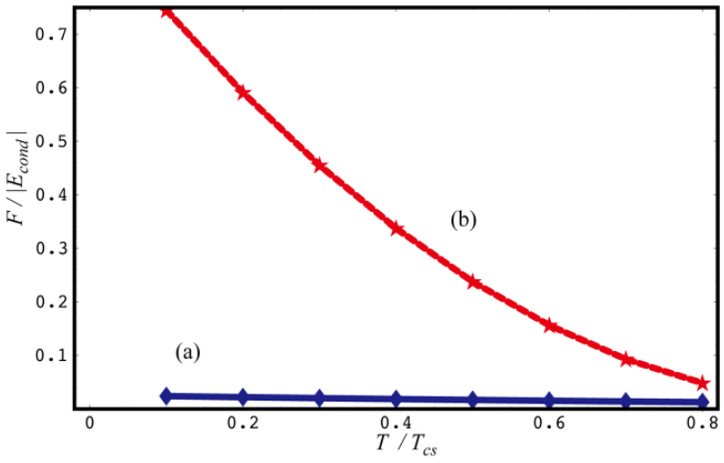

Figure 15. Free energies of (a) the most stable state (udud) and (b) an excited state (uudd). E_{cond} is the condensation energy of the superconductor and T_{cs} is the critical temperature of the s-wave superconductor.

Second property is the stability of the degenerate stable states. For the square d-dots, most stable states show antiferromagnetic order of spontaneous magnetic fluxes, and we call these state udud (up down up down) (Fig. 4 (a)). There are other states, which have higher free energy. In Fig. 14 (b), one of such states is shown. In this state, spontaneous magnetic fluxes do not show antiferromagnetic order, but parallel magnetic fluxes align at the upper or lower edges. We call this state uudd (up up down down). The free energies of the udud and uudd states are shown in Fig. 15. Well below the critical temperature of the s-wave superconductor T_{cs}, free energy difference between udud (a) and uudd (b) states becomes comparable to the condensation energy of the superconductor. Therefore we can treat them as two-level systems.

4. Interaction between d-dots

As shown in previous section, the d-dots have double degenerate stable states. So we can use them as bits or 1/2 spins. In order to use them as artificial spins, the d-dots will be placed periodically or randomly. Then the interaction between them is important for these spin systems. For using the d-dots as computational bits, they are also placed to transform the information. Therefore interaction between d-dots also important for these applications.

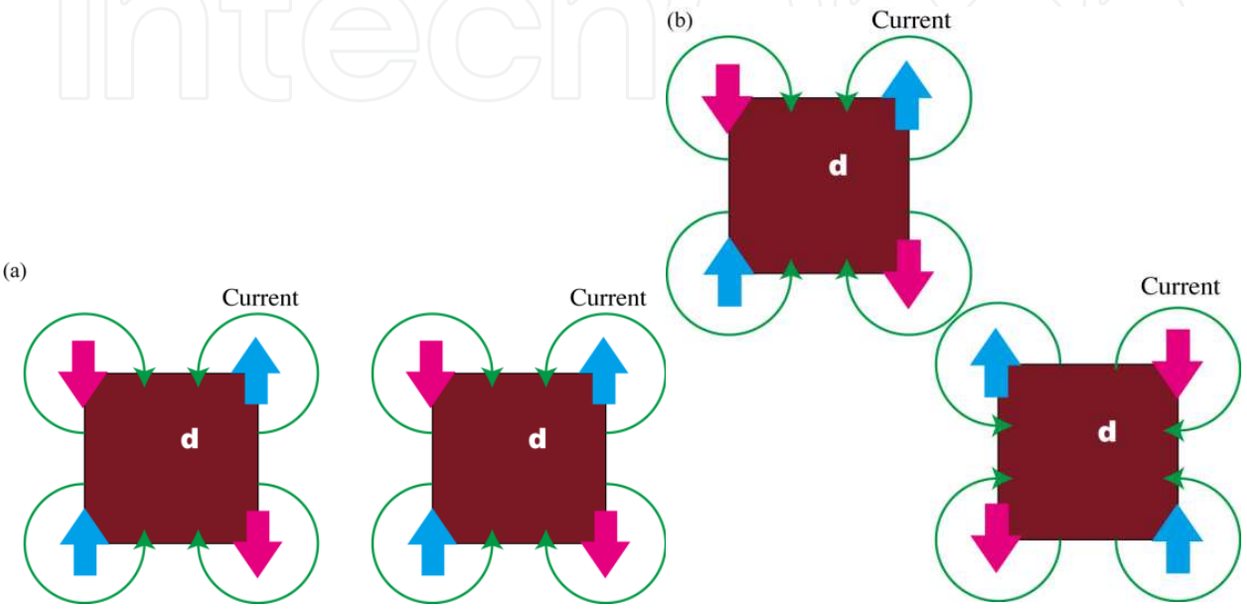

Figure 16. Pairs of d-dots in a parallel (a) or a diagonal (b) positions.

How the d-dots interact with each other? Interaction between d-dots basically comes from the interaction between spontaneous magnetic fluxes or vortices. If the spontaneous vortices are independent from each other, that is, if there is no current flow between the vortices, then via a purely electromagnetic interaction, they interact. This is the case of the π-ring system of Kirtley et al. [4]. If the vortices are interacting in the same superconductors, there is a supercurrent flow around the vortices and ordinary vortices interact with each other through this current. The current distribution around a singly quantized vortex is given by the first order Bessel function. And therefore the interaction force to vortex 1 from vortex 2 is given as,

$$\mathbf{f}_{12} = \frac{(\boldsymbol{\Phi}_0)_1 (\boldsymbol{\Phi}_0)_2}{8\pi^2 \lambda^3} K_1\left(\frac{r_{12}}{\lambda}\right)\hat{\mathbf{r}}_{12} \tag{24}$$

Where r_{12} and $\hat{\mathbf{r}}_{12}$ are distance between two vortices and a unit vector from the vortex 2 to the vortex 1, respectively, and K_1 is the first order modified Bessel function. Directions of vortices are expressed by $(\boldsymbol{\Phi}_0)_i$ and if two vortices are parallel (anti-parallel) then interaction is repulsive (attractive), respectively.

For d-dots, there is an s-wave region between d-wave islands, and the spontaneous currents around the corners affect each other as usual supercurrent around singly quantized vortices,

mentioned above. Then, an interaction between d-dots arises through the spontaneous currents in the s-wave region. If two square d-dots are in a line (Fig. 16 (a)), nearest vortex pair should be antiparallel (e.g. right-upper flux in the left d-dot and left upper vortex in the right d-dot should be antiparallel). And then we can expect that two d-dots will have a same spontaneous magnetic flux distribution, as shown in Fig. 16 (a). Therefore when we regard a d-dot as a spin, they interact ferromagnetically. In contrast to this configuration, if two square d-dots are placed diagonally (Fig. 16 (b)), then we expect an antiferromagnetic interaction by the same argument. In Fig. 17, stable states for parallel two d-dots are shown. For short distance ((e)), the nearest magnetic fluxes disappear and the flux distributions of two d-dots are same. Increasing the distance, the nearest magnetic fluxes appear and becomes gradually large ((f)-(h)) and the states of the d-dots are still same.Therefore ferromagnetic states are always stable, as we expected, and this is independent from the distance.

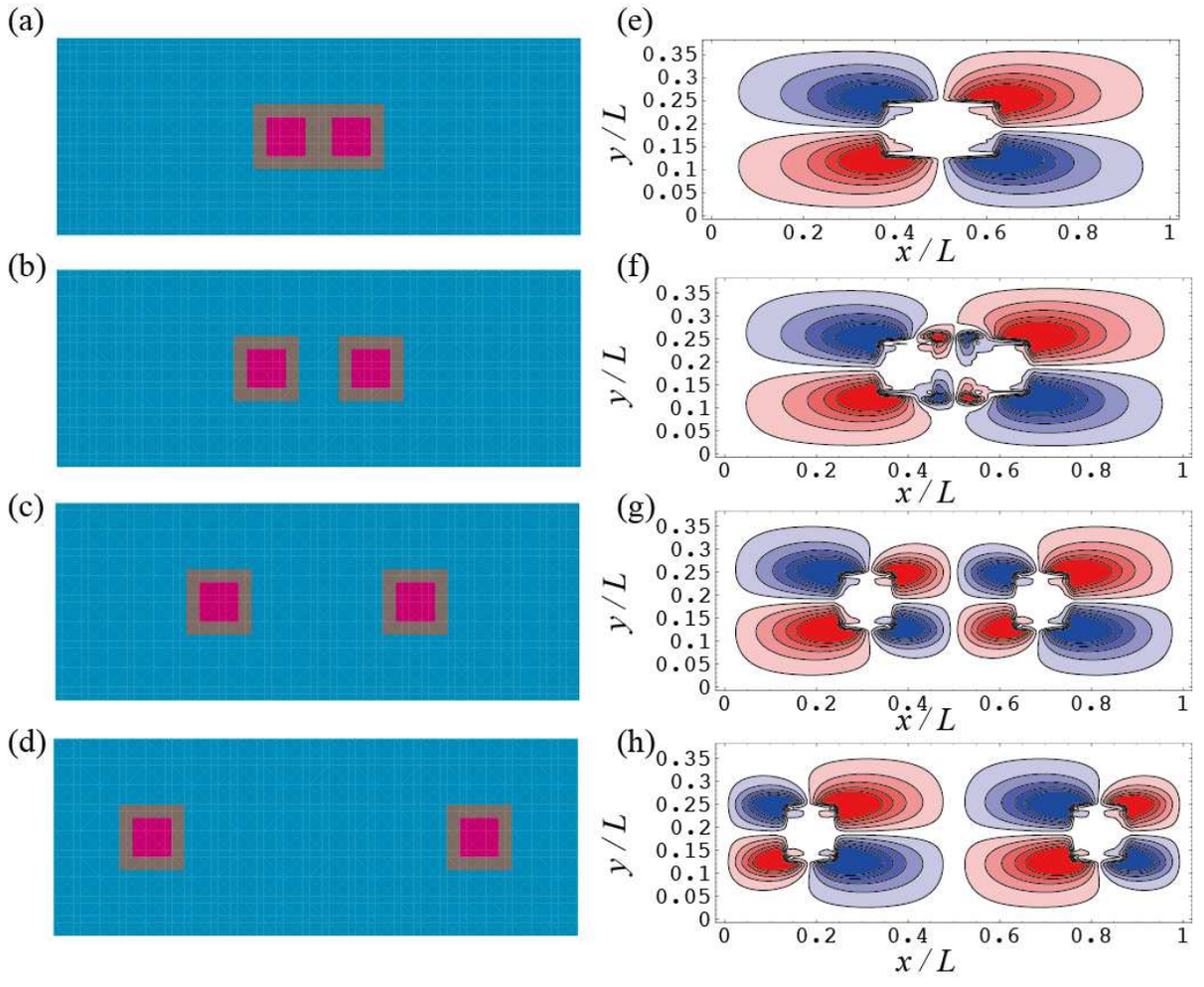

Figure 17. Stable states for parallel two d-dots. (a)-(d) : configurations of d- and s-wave superconductors. (e)-(h): Stable magnetic field distributions.

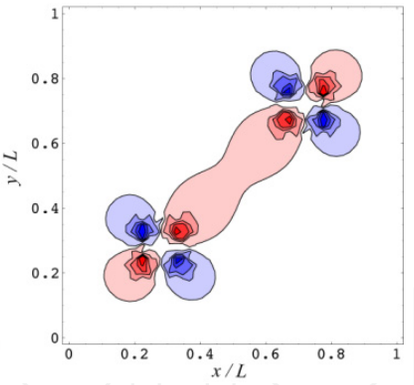

Figure 18. Stable magnetic field distribution around a pair of d-dots, which are placed diagonally. The states of these d-dots are same and therefore they interact ferromagnetically.

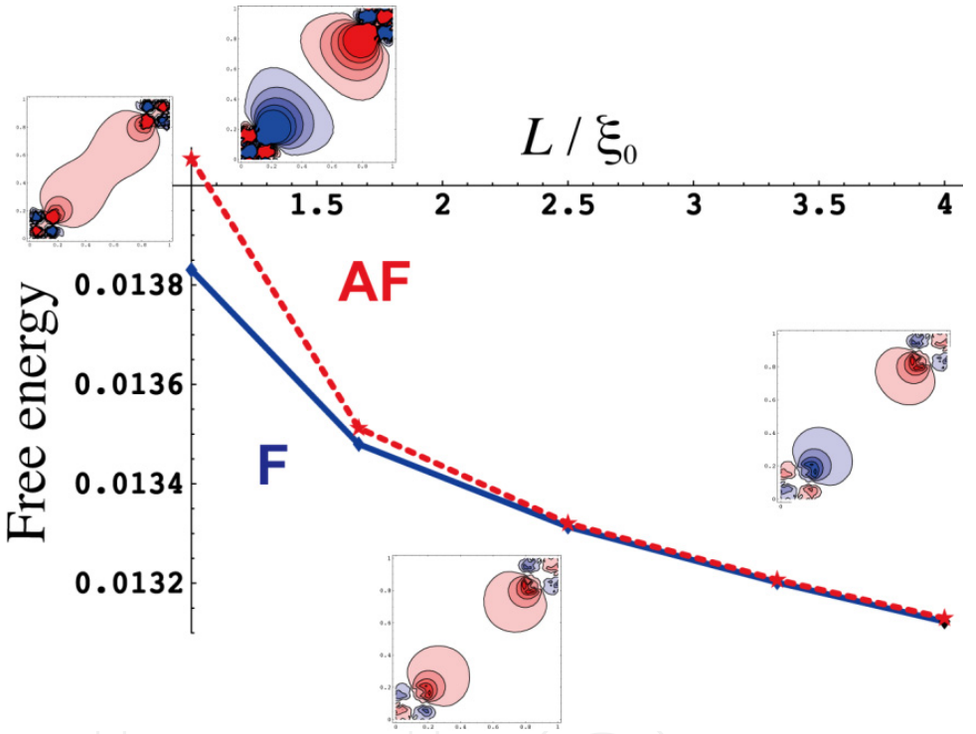

Figure 19. Free energies for Ferromagnetic (F) and Antiferromagnetic states in diagonally placed two d-dots.

However, for diagonally placed two d-dots, the magnetic field distribution is not so simple. In Fig. 18, the stable state is shown for short distance between two diagonally placed d-dots. Unlike to the expectation from the usual vortex-vortex interaction, ferromagnetic state becomes stable. This is because two adjacent half-quantum fluxes are connected and form broad single quantum flux and this can occur when two fluxes are parallel. Therefore the ferromagnetic state becomes stable. It seems that the energy of this configuration becomes lower when two half-quantum fluxes are closer to each other. This property does not appear for ordinary vortices and we call this a fusion of half-quantum vortices. In Fig. 19, distance dependence of the free energies for the ferromagnetic and antiferromagnetic states are plotted. When distance between two d-dots is short, the ferromagnetic state has much lower

free energy than that of the antiferromagnetic state. For longer distance, free energies of these states are almost same, because the spontaneous magnetic fluxes become almost independent as shown in the insets of Fig. 19.

These interactions between d-dots can be used for changing the state of the d-dots [26]. Using these interactions, the d-dots have a potential applicability to the superconducting devices[27].

5. Conclusions

We showed that the anisotropic pairing of superconductivity causesinteresting phenomena when two different superconductors are combined. Spontaneous half-quantized magnetic flux around the junction between d-wave and s-wave superconductors is one of such phenomena. It is simulated by the two-components Ginzburg-Landau equations, which can treat the anisotropy of d-wave superconductivity. This half-quantum magnetic state for the d-wave superconductors embedded in the s-wave superconductor has good properties for applications to superconducting devices, especially for classical bits or qubits.

Appendix

In this appendix, the coefficients in Eqs. 13-18 aregiven. For d-wave superconducting regions, they are defined as,

$$P_{ij}^{dd}\left(\{\mathbf{A}\}\right)\equiv\frac{3}{4}\xi_d^2\left(\Delta_d^0\right)^2\left(\sum_{\alpha=x,y}K_{ij}^{\alpha\alpha}+\sum_{\substack{i_1i_2\\ \alpha=x,y}}I_{i_1i_2ij}A_{i_1\alpha}A_{i_2\alpha}\right)-\frac{3}{4}\left(\Delta_d^0\right)^2 I_{ij} \tag{25}$$

$$\begin{aligned}P_{ij}^{dd\,2R}\left(\{\Delta\}\right)&\equiv\left(\frac{\lambda_s}{\lambda_d}\right)^2\sum_{i_1i_2}I_{i_1i_2ij}\left(3\,\mathrm{Re}\,\Delta_{si_1}\,\mathrm{Re}\,\Delta_{si_2}+\mathrm{Im}\,\Delta_{si_1}\,\mathrm{Im}\,\Delta_{si_2}\right)\\&+\frac{3}{4}\sum_{i_1i_2}I_{i_1i_2ij}\left(3\,\mathrm{Re}\,\Delta_{di_1}\,\mathrm{Re}\,\Delta_{di_2}+\mathrm{Im}\,\Delta_{di_1}\,\mathrm{Im}\,\Delta_{di_2}\right)\end{aligned} \tag{26}$$

$$\begin{aligned}P_{ij}^{dd\,2I}\left(\{\Delta\}\right)&\equiv\left(\frac{\lambda_s}{\lambda_d}\right)^2\sum_{i_1i_2}I_{i_1i_2ij}\left(\mathrm{Re}\,\Delta_{si_1}\,\mathrm{Re}\,\Delta_{si_2}+3\,\mathrm{Im}\,\Delta_{si_1}\,\mathrm{Im}\,\Delta_{si_2}\right)\\&+\frac{3}{4}\sum_{i_1i_2}I_{i_1i_2ij}\left(\mathrm{Re}\,\Delta_{di_1}\,\mathrm{Re}\,\Delta_{di_2}+3\,\mathrm{Im}\,\Delta_{di_1}\,\mathrm{Im}\,\Delta_{di_2}\right)\end{aligned} \tag{27}$$

$$Q_{ij}^{dd}\left(\{\mathbf{A}\}\right)\equiv-\frac{3}{4}\xi_d^2\left(\Delta_d^0\right)^2\sum_{\substack{i_1\\ \alpha=x,y}}\left(J_{ii_1j}^{\alpha}-J_{ji_1i}^{\alpha}\right)A_{i_1}^{\alpha} \tag{28}$$

$$Q_{ij}^{dd\,2}\left(\{\Delta\}\right)\equiv\left(\frac{\lambda_s}{\lambda_d}\right)^2\sum_{i_1i_2}I_{i_1i_2ij}\,2\,\mathrm{Im}\,\Delta_{si_1}\,\mathrm{Re}\,\Delta_{si_2}+\frac{3}{4}\sum_{i_1i_2}I_{i_1i_2ij}\,2\,\mathrm{Im}\,\Delta_{di_1}\,\mathrm{Re}\,\Delta_{di_2} \tag{29}$$

$$P_{ij}^{ds}\left(\{\mathbf{A}\}\right)\equiv\frac{3}{4}\xi_d^2\left(\Delta_d^0\right)^2\frac{\lambda_s}{\lambda_d}\left(K_{ij}^{xx}-K_{ij}^{yy}+\sum_{\substack{i_1i_2\\ \alpha=x,y}}I_{i_1i_2ij}\left(A_{i_1x}A_{i_2x}-A_{i_1y}A_{i_2y}\right)\right) \tag{30}$$

$$Q_{ij}^{ds}\left(\{\mathbf{A}\}\right)\equiv\frac{3}{4}\xi_d^2\left(\Delta_d^0\right)^2\frac{\lambda_s}{\lambda_d}\sum_{i_1}\left\{\left(J_{ii_1j}^{x}-J_{ji_1i}^{x}\right)A_{i_1}^{x}-\left(J_{ii_1j}^{y}-J_{ji_1i}^{y}\right)A_{i_1}^{y}\right\} \tag{31}$$

$$V_i^{dR}\left(\{\Delta\}\right)\equiv\frac{3}{2}\sum_{i_1i_2i_3}I_{i_1i_2i_2i}\Delta_{i_1}\Delta_{i_2}^{*}\,\mathrm{Re}\,\Delta_{i_3} \tag{32}$$

$$V_i^{dI}\left(\{\Delta\}\right)\equiv\frac{3}{2}\sum_{i_1i_2i_3}I_{i_1i_2i_2i}\Delta_{i_1}\Delta_{i_2}^{*}\,\mathrm{Im}\,\Delta_{i_3} \tag{33}$$

$$P_{ij}^{ss}\left(\{\mathbf{A}\}\right)\equiv\frac{3}{2}\xi_d^2\left(\Delta_d^0\right)^2\left(\frac{\lambda_s}{\lambda_d}\right)^2\left(\sum_{\alpha=x,y}K_{ij}^{\alpha\alpha}+\sum_{\substack{i_1i_2\\ \alpha=x,y}}I_{i_1i_2ij}A_{i_1\alpha}A_{i_2\alpha}\right)+2\left(\frac{\lambda_s}{\lambda_d}\right)^4\left(\Delta_s^0\right)^2I_{ij} \tag{34}$$

$$\begin{aligned}P_{ij}^{ss2R}\left(\{\Delta\}\right)&\equiv\left(\frac{\lambda_s}{\lambda_d}\right)^2\sum_{i_1i_2}I_{i_1i_2ij}\left(3\,\mathrm{Re}\,\Delta_{di_1}\,\mathrm{Re}\,\Delta_{di_2}+\mathrm{Im}\,\Delta_{di_1}\,\mathrm{Im}\,\Delta_{di_2}\right)\\&+2\left(\frac{\lambda_s}{\lambda_d}\right)^4\sum_{i_1i_2}I_{i_1i_2ij}\left(3\,\mathrm{Re}\,\Delta_{si_1}\,\mathrm{Re}\,\Delta_{si_2}+\mathrm{Im}\,\Delta_{si_1}\,\mathrm{Im}\,\Delta_{si_2}\right)\end{aligned} \tag{35}$$

$$\begin{aligned}P_{ij}^{ss2I}\left(\{\Delta\}\right)&\equiv\left(\frac{\lambda_s}{\lambda_d}\right)^2\sum_{i_1i_2}I_{i_1i_2ij}\left(\mathrm{Re}\,\Delta_{di_1}\,\mathrm{Re}\,\Delta_{di_2}+3\,\mathrm{Im}\,\Delta_{di_1}\,\mathrm{Im}\,\Delta_{di_2}\right)\\&+2\left(\frac{\lambda_s}{\lambda_d}\right)^4\sum_{i_1i_2}I_{i_1i_2ij}\left(\mathrm{Re}\,\Delta_{si_1}\,\mathrm{Re}\,\Delta_{si_2}+3\,\mathrm{Im}\,\Delta_{si_1}\,\mathrm{Im}\,\Delta_{si_2}\right)\end{aligned} \tag{36}$$

$$Q_{ij}^{ss}\left(\{\mathbf{A}\}\right)\equiv-\frac{3}{2}\xi_d^2\left(\Delta_d^0\right)^2\left(\frac{\lambda_s}{\lambda_d}\right)^2\sum_{\substack{i_1\\ \alpha=x,y}}\left(J_{ii_1j}^{\alpha}-J_{ji_1i}^{\alpha}\right)A_{i_1}^{\alpha} \tag{37}$$

$$Q_{ij}^{ss2}\left(\{\Delta\}\right)\equiv\left(\frac{\lambda_s}{\lambda_d}\right)^2\sum_{i_1i_2}I_{i_1i_2ij}\,2\,\mathrm{Im}\,\Delta_{di_1}\,\mathrm{Re}\,\Delta_{di_2}+2\left(\frac{\lambda_s}{\lambda_d}\right)^4\sum_{i_1i_2}I_{i_1i_2ij}\,2\,\mathrm{Im}\,\Delta_{si_1}\,\mathrm{Re}\,\Delta_{si_2} \tag{38}$$

$$V_i^{sR}\left(\{\Delta\}\right)\equiv4\left(\frac{\lambda_s}{\lambda_d}\right)^4\sum_{i_1i_2i_3}I_{i_1i_2i_2i}\Delta_{si_1}\Delta_{si_2}^{*}\,\mathrm{Re}\,\Delta_{si_3} \tag{39}$$

$$V_i^{sI}\left(\{\Delta\}\right)\equiv4\left(\frac{\lambda_s}{\lambda_d}\right)^4\sum_{i_1i_2i_3}I_{i_1i_2i_2i}\Delta_{si_1}\Delta_{si_2}^{*}\,\mathrm{Im}\,\Delta_{si_3} \tag{40}$$

For s-wave superconducting regions, they are defined similarly.

The coefficients in Eqs. 17 and 18 in the d-wave superconducting region are given as,

$$R_{ij}\left(\{\mathbf{A}\}\right) \equiv \frac{3}{2}\kappa_d^2\xi_d^2\left(\Delta_d^0\right)^2\left(\sum_{\alpha=x,y} K_{ij}^{\alpha\alpha}\right)+\frac{3}{4}\sum_{i_1 i_2} I_{i_1 i_2 ij}\left[2\,\mathrm{Re}\left(\Delta_{di_1}\Delta_{di_2}^*\right)+4\left(\frac{\lambda_s}{\lambda_d}\right)^2\mathrm{Re}\left(\Delta_{si_1}\Delta_{si_2}^*\right)\right], \tag{41}$$

$$R_{ij}^2\left(\{\mathbf{A}\}\right) \equiv 3\sum_{i_1 i_2} I_{i_1 i_2 ij}\left[\left(\frac{\lambda_s}{\lambda_d}\right)\mathrm{Re}\left(\Delta_{di_1}^*\Delta_{si_2}\right)\right], \tag{42}$$

$$S_{ij} \equiv \frac{3}{2}\kappa_d^2\xi^2\left(\Delta_d^0\right)^2\left(K_{ij}^{xy}-K_{ij}^{yx}\right), \tag{43}$$

$$T_i^{\alpha} \equiv \frac{3}{2}\sum_{i_1 i_2} J_{i_1 i_2 i}^{\alpha}\left[\mathrm{Im}\left(\Delta_{di_1}^*\Delta_{di_2}\right)+2\left(\frac{\lambda_s}{\lambda_d}\right)^2\mathrm{Re}\left(\Delta_{si_1}^*\Delta_{si_2}\right)\right]\ (\alpha=x,y), \tag{44}$$

$$T_i^{2\alpha} \equiv \frac{3}{2}\sum_{i_1 i_2} J_{i_1 i_2 i}^{\alpha}\left(\frac{\lambda_s}{\lambda_d}\right)\left[\mathrm{Im}\left(\Delta_{di_1}^*\Delta_{si_2}\right)+\mathrm{Im}\left(\Delta_{si_1}^*\Delta_{di_2}\right)\right]\ (\alpha=x,y), \tag{45}$$

$$U_i^{\alpha} \equiv \frac{3}{4}\kappa_d^2\xi_d^2\left(\Delta_d^0\right)^2\frac{2\pi}{\Phi_0}HJ_i^{\alpha}\ (\alpha=x,y). \tag{46}$$

Author details

Masaru Kato
Department of Mathematical Sciences, Osaka Prefecture University1-1, Gakuencho, Sakai, Osaka, Japan

Takekazu Ishida
Department of Physics and Electronics, Osaka Prefecture University, 1-1, Gakuencho, Sakai, Osaka, Japan

Tomio Koyama
Institute of Material Sciences, Tohoku University, Sendai, Japan

Masahiko Machida
CCSE, Japan Atomic Energy Agency, Tokyo, Japan

Acknowledgement

One of the authors (M. K.) thanks his former and present graduate students, M. Ako, M. Hirayama, S. Nakajima, H. Suematsu, T.Minamino, S. Tomita, Y. Niwa, and D. Fujibayashi for useful discussions. This work is partly supported by "The Faculty Innovation Research Project" of Osaka Prefecture University and it was supported by the CREST-JST project.

6. References

[1] Tinkham M. Introduction to Superconductivity. New York: McGrawa-Hill, inc; 1996.
[2] Sigrist M, Ueda K. Rev. Mod. Phys. 1991; 63(2): 239-311.
[3] Tsuneto T. Superconductivity and Superfluidity. Cambridge: Cambridge University Press; 1998.
[4] Tsuei C C, Kirtley J R. Pairing symmetry in cuprate superconductors. Rev. Mod. Phys. 2000;72(4): 969-1016.
[5] Van Harlingen D J. Phase-sensitive tests of the symmetry of the pairing state in the high-temperature superconductors—Evidence for dx2-y2 symmetry.Rev. Mod. Phys. 1995;67(2): 515-535.
[6] Hilgenkamp A, Ariando, Smilde H-J H, Blank D H A, Rijnders G, Rogalla H, Kirtley J R, Tsuei C C. Ordering and manipulation of the magnetic moments in large-scale superconducting -loop arrays. Nature 2003; 422, 50 -53.
http://www.nature.com/nature/journal/v422/n6927/full/nature01442.html
[7] Kirtley J R, Tsuei C C, Ariando, Smilde H-J H, Hilgenkamp H. Antiferromagnetic ordering in arrays of superconducting π-rings. Phys. Rev. B 2005; 72 (21): 214521 (1-11).
[8] IoffeL B, Geshkenbein V B, Feigel'man M V, Fauchère A L, Blatter G. Environmentally decoupled sds -wave Josephson junctions for quantum computing. Nature 1999; 398: 679-681.
[9] KatoM, AkoM, MachidaM,Koyama T, IshidaT.Ginzburg–Landau calculations of d-wave superconducting dot in s-wave superconducting matrix. Physica C 2004; 412-414: 352-357.
[10] Kato M, Ako M, Machida M, Koyama T, Ishida T. Structure of magnetic flux in nano-scaled superconductors. J. Mag. Mag. Mat. 2004; 272-276, 171-172.
[11] Ako M, Ishida T, Machida M, Koyama T, Kato M. Vortex state of nano-scaled superconducting complex structures (d-dot).Physica C 2004; 412-414: 544-547.
[12] Ren Y, Xu J-H, Ting C S. Ginzburg-Landau Equations and Vortex Structure of a dx2-y2 Superconductor. Phys. Rev. Lett. 1995;74: 3680-3683.
[13] Xu J H, Ren Y, Ting C S. Ginzburg-Landau equations for a d-wave superconductor with applications to vortex structure and surface problems. Phys. Rev. B 1995; 52:7663-7674.
[14] XuJ H, RenY, Ting C S.Structures of single vortex and vortex lattice in a d-wave superconductor. Phys. Rev. B 1996; 53:R2991-R2994.
[15] Li Q, Wang Z D, Wang Q H. Vortex structure for a d+is-wave superconductor. Phys. Rev. B; 1999; 59:613-618.
[16] Garg A. Ginzhurg-Landau Theory of the Phase Diagram of Superconducting UPt_3. Phys. Rev. Lett. 1992; 69: 676-679.
[17] Garg A, Chen D-C. Two-order-parameter theory of the phase diagram of superconducting UPt_3. Phys. Rev. B 1994;49: 479-493.
[18] Martisovits V, Zaránd G, Cox D L. Theory of "Ferrisuperconductivity" in $U_{1-x}Th_xBe_{13}$. Phys. Rev. Lett. 2000; 84: 5872-5875.
[19] Wang Q H, Wang Z D. Vortex flow in a two-component unconventional superconductor. Phys. Rev. B 1998; 57: 10307-10310.

[20] Agterberg D F. Square vortex lattices for two-component superconducting order parameters. Phys. Rev. 1998; 58; 14484-14489.
[21] Babaev E, Speight M. Semi-Meissner state and neither type-I nor type-II superconductivity in multicomponent superconductors. Phys. Rev. B 2005; 72; 180502(R)1-4.
[22] Dao V H, Chibotaru L F, Nishio T, Moshchalkov V V. Giant vortices, rings of vortices, and reentrantbehavior in type-1.5 superconductors. Phys. Rev. B 2011; 83: 020503 (R) 1-4.
[23] Du Q, Gunzburger M D, Peterson J S. Analysis and approximation of the Ginzburg Landau model of superconductivity. SIAM Rev. 1992;34:54-81.
[24] Du Q, Gunzburger M D, Peterson J S.Solving the Ginzburg-Landau equations by finite-element methods. Phys. Rev. B1992; 46: 9027-9034.
[25] Wang Z D, Wang Q H. Vortex state and dynamics of a d-wave superconductor: Finite-element analysis; Phys. Rev. B 1997; 55: 11756-11765.
[26] Nakajima S, Kato M, Koyama T, Machida M, Ishida T,Nori F. Simulation of logic gate using d-dot's.PhysicaC 2008; 468: 769-772.
[27] Koyama T, Machida M, Kato M, Ishida T. Quantum theory for the Josephson phase dynamics in a d-dot. Physica C 2005; 426-431: 1561-1565.